# Influence of Pseudohalide Ions on the Molecular Structure and Magnetic Properties of the Manganese(II)−Bipyrimidine−Pseudohalide System

**Roberto Cortés,*,† M. Karmele Urtiaga,‡ Luis Lezama,§ J. Luis Pizarro,‡ M. Isabel Arriortua,‡ and Teófilo Rojo*,§**

Departamento de Química Inorgánica, Universidad del País Vasco, Aptdo. 450, E-01080 Vitoria, Spain, and Aptdo. 644, E-48080 Bilbao, Spain, and Departamento de Mineralogía-Petrología, Universidad del País Vasco, Aptdo. 644, E-48080 Bilbao, Spain

*Received August 8, 1996*[⊗]

The compounds $[Mn_2(bpm)_3(NCS)_4]$ (**1**), $[Mn(bpm)(NCO)_2]$ (**2**), and $[Mn_2(bpm)(N_3)_4]$ (**3**) (where bpm= 2,2′-bipyrimidine) have been synthesized and characterized. Compound **1** crystallizes in the triclinic $P\bar{1}$ space group, with $a = 9.122(1)$ Å, $b = 9.229(1)$ Å, $c = 11.710(2)$ Å, $\alpha = 74.89(1)°$, $\beta = 80.30(1)°$, $\gamma = 61.04(1)°$, $V = 831.7(2)$ Å$^3$, $Z = 2$, $R(F_o) = 0.029$, and $wR(F_o^2) = 0.078$. Compound **2** crystallizes in the monoclinic $C2/c$ space group, with $a = 7.309(1)$ Å, $b = 14.498(2)$ Å, $c = 10.740(4)$ Å, $\beta = 99.93(4)°$, $V = 1121.0(5)$ Å$^3$, $Z = 4$, $R = 0.025$, and $wR(F_o^2) = 0.060$. In the case of compound **3**, the crystal parameters of the monoclinic $C2/m$ space group are $a = 6.206(2)$ Å, $b = 15.084(2)$ Å, $c = 8.909(1)$ Å, $\beta = 95.75(2)°$, $V = 829.8(3)$ Å$^3$, $Z = 4$, $R = 0.029$, and $wR(F_o^2) = 0.069$. The pseudohalide ions have a dramatic influence in the molecular structures of the three compounds. Compound **1** is dinuclear, with the manganese(II) ions bridged by bpm ligands and with terminal bpm and NCS groups; compound **2** is a linear chain of manganese(II) ions bridged by bpm ligands in *cis* conformation, with terminal cyanate groups; compound **3** shows a two-dimensional honeycomb like structure, where the sheets consist of an infinite hexagonal array of manganese(II) ions bridged by bischelating bpm ligands and double end-on azido bridges. The manganese(II) ions have octahedral environments in all cases. Magnetic susceptibility measurements show antiferromagnetic couplings for compounds **1** and **2**, while alternating ferro-antiferromagnetism is observed for compound **3**. The obtained exchange parameters are $J = -0.72$ K and $J = -0.78$ K for compounds **1** and **2**, respectively. No theoretical model is available for compound **3**, which represent the first two-dimensional honeycomb-like compound showing alternating signs in the magnetic interactions.

## Introduction

In the recent years, the work developed by our group on pseudohalide-bridged magnetic molecular compounds has led to systems of increasing nuclearity.[1−3] It is well-known that one-dimensional systems show no magnetic ordering, except at absolute zero, owing to the very weak interchain interactions compared with the intrachain ones. Therefore, increasing in dimensionality is a necessary factor to obtain high magnetic ordering. On the other hand, systems with magnetic interactions alternating in sign are very scarce and only one-dimensional compounds are known.[4]

The pseudohalide ions, specially the azido one, have been shown as good bridging ligands for obtaining magnetic molecular compounds of high nuclearity.[5−7] Magneto-structural studies have shown that the end-to-end (EE) azido and end-on (EO) azido and cyanate bridging modes are able to mediate antiferromagnetic[8] and ferromagnetic[9,10] interactions, respectively. Theoretical calculations have revealed that the singlet and triplet ground states are favored for the EE and EO modes, respectively. The spin polarization theory[11] has recurrently been used to explain the ferromagnetic interactions observed in the EO-bridged azido systems. However, a recent report[12] of a polarized neutron diffraction study on $[Cu_2(t\text{-}bupy)_4(\mu_2\text{-}1,1\text{-}N_3)](ClO_4)_2$ revealed spin density calculations that contradict the theoretical interpretation involving spin polarization theory.

The 2,2′-bipyrimidine ligand, in the bischelating coordination mode, has been shown as a useful tool for connecting different metals, transmitting antiferromagnetic interactions, and for obtaining magnetic systems of high nuclearity. In this way,

† Dept. de Química Inorgánica, Facultad de Farmacia, Vitoria.
‡ Dept. Mineralogía-Petrología, Facultad de Ciencias, Bilbao.
§ Dept. de Química Inorgánica, Facultad de Ciencias, Bilbao.
⊗ Abstract published in *Advance ACS Abstracts,* September 15, 1997.

(1) (a) Cortés, R.; Urtiaga, M. K.; Lezama, L.; Pizarro, J. L.; Goñi, A.; Arriortua, M. I.; Rojo, T. *Inorg. Chem.* **1994**, *33*, 4009. (b) Cortés, R.; Lezama, L.; Pizarro, J. L.; Arriortua, M. I.; Solans, X.; Rojo, T. *Angew. Chem., Int. Ed. Engl.* **1994**, *33*, 2488.
(2) Cortés, R.; Lezama, L.; Pizarro, J. L.; Arriortua, M. I.; Rojo, T. *Angew. Chem., Int. Ed. Engl.* **1996**, *in press*.
(3) Mautner, F. A.; Cortés, R.; Lezama, L.; Rojo, T. *Angew. Chem., Int. Ed. Engl.* **1996**, *35*, 78.
(4) (a) De Groot, H. J. M.; de Jongh, L. J.; Willet, R. D.; Reedijk, J. *J. Appl. Phys.* **1982**, *53*, 8038. (b) Benelli, C.; Gatteschi, D.; Carnegie, D. W.; Carlin, R. L. *J. Am. Chem. Soc.* **1985**, *107*, 2560. (c) De Munno, G.; Julve, M.; LLoret, F.; Faus, J.; Verdaguer, M.; Caneschi, A. *Angew. Chem., Int. Ed. Engl.* **1993**, *32*, 1046. (d) Vasilevesky, I.; Rose, N. R.; Stenkamp, R.; Willet, R. D. *Inorg. Chem.* **1991**, *30*, 4082.
(5) (a) Pierpont, C. G.; Hendrickson, D. N.; Duggan, D. M.; Wagner, F.; Barefield, E. K. *Inorg. Chem.* **1975**, *14*, 604. (b) Escuer, A.; Vicente, R.; Ribas, J.; El Fallah, M. S.; Solans, X.; Font-Bardía, M. *Inorg. Chem.* **1993**, *32*, 3727.
(6) (a) Ribas, J.; Monfort, M.; Solans, X.; Drillon, M. *Inorg. Chem.* **1994**, *33*, 742. (b) Goher, M. A. S.; Mautner, F. A. *Croat. Chem. Acta* **1990**, *63*, 559.
(7) Escuer, A.; Vicente, R.; Goher, M. A. S.; Mautner, F. A. *Inorg. Chem.* **1995**, *34*, 5707.
(8) Duggan, D. M.; Hendrickson, D. N. *Inorg. Chem.* **1973**, *12*, 2422.
(9) (a) Commarmond, J.; Plumere, P.; Lehn, J. M.; Agnus, Y.; Louis, R.; Weiss, R.; Kahn, O.; Morgenstern-Badarau, I. *J. Am. Chem. Soc.* **1982**, *104*, 6330. (b) Sikorav, R. E.; Bkouche-Waksman. I.; Kahn, O. *Inorg. Chem.* **1984**, *23*, 490.
(10) Arriortua, M. I.; Cortés, R.; Mesa, J. L.; Lezama, L.; Rojo, T.; Villeneuve, G. *Transition Met. Chem.* **1988**, *13*, 371.
(11) (a) Kahn, O. *Comments Inorg. Chem.* **1984**, *3*, 105. (b) Charlot, M. F.; Kahn, O.; Chaillet, M.; Larrieu, C. *J. Am. Chem. Soc.* **1986**, *108*, 2574.
(12) Aebersold, M.; Bergerat, P.; Gillon, B.; Kahn, O.; Pardi, L.; Tukzet, F.; Öhrström, L.; Grand, A. *NATO Advanced Research Workshop on Magnetism-A Supramolecular Function*; Carcans-Maubuisson, France, Sept 16−21, 1995.

S0020-1669(96)00969-X CCC: $14.00 

1D, 2D, and 3D systems,[13] chains with interactions alternating in sign,[1c] and new honeycomb layered materials have been obtained.[14] This ligand could, therefore, be a good candidate to attempt the connection of one-dimensional compounds and thus to obtain systems of higher dimensionality.

If we take into account the ability of the EO pseudohalide bridging and the bpm ligand to mediate ferromagnetic and antiferromagnetic interactions, respectively a combination of both pseudohalide and bpm ligands could, therefore, give rise to the attainment of desired high dimensional compounds. Following this method we have isolated and structurally characterized the dinuclear compound **1**, the one-dimensional compound **2**, and the sheetlike polymer **3**. Magnetic measurements for both compounds **1** and **2** indicate an antiferromagnetic coupling between the manganese(II) ions, while alternating ferro-antiferromagnetic interactions are observed for compound **3**, which represent the first two-dimensional compound showing this kind of magnetic alternation. A preliminary communication has been published for compound **3**.[2] Considering the strong pseudo-c symmetry observed for this compound, it was recrystallized, new diffraction data were collected, and the structure was solved again within a *C*2/*m* space group.

## Experimental Section

**Materials.** 2,2′-Bipyrimidine (Merck), manganese(II) nitrate (Aldrich), potassium thiocyanate (Sigma), potassium cyanate (Sigma), and sodium azide (Sigma) were purchased and used without further purification.

**Synthesis. Caution!** *Azide metal complexes are potentially explosive. Only a small amount of material should be prepared, and it should be handled with caution.*

**Synthesis of Compounds 1−3.** The three compounds were prepared in the same way by treating aqueous/methanolic solutions (20 mL) containing manganese(II) nitrate and the respective pseudohalide salt with 2,2′-bipyrimidine in 1/2/0.5 proportion. The samples were stirred without heating for about 2 h and left standing. Slow evaporation of the resulting solutions at room temperature gave orange-yellow prisms for compounds **1** and **2**, while yellow-orange needle-prisms were obtained for compound **3**. The latter compound was recrystallized in the same solving medium to obtain better X-ray-quality crystals.

The compounds were satisfactorily analized for C, H, and N with the formulas $C_{28}H_{18}N_{16}S_4Mn_2$, $C_{10}H_6N_6O_2Mn$ and $C_8H_6N_{16}Mn_2$ for **1**−**3**, respectively.

**Physical Measurements.** IR spectra were recorded on a Nicolet 520 FTIR spectrophotometer in the 400−4000 $cm^{-1}$ region. Magnetic susceptibilities of powdered samples were carried out in the temperature range 1.8−300 K using a Quantum Design Squid magnetometer, equipped with a helium continuous-flow cryostat. The magnetic field was approximately 1000 G, a field at which the *M* vs *H* curve is linear even for a temperature of 1.8 K. The experimental susceptibilities were corrected for the diamagnetism of the constituent atoms (Pascal tables).

**X-ray Structural Determinations.** Diffraction data for **1**−**3** were collected at room temperature on an Enraf-Nonius CAD4 automated diffractometer using graphite-monochromated Mo Kα radiation ($\lambda$ = 0.710 69 Å). Details on crystal data, intensity collection, and some features of the structure refinement for the three compounds are reported in Table 1. Lattice constants were obtained by a least-squares fit of 25 reflections in the range $8° < \theta < 12°$. The intensities of three standard reflections were measured every 2 h and showed no significant decrease in intensity.

For compound **1**, 5116 reflections were measured in the range $1.8 \le \theta \le 30°$, and 4831 reflections are assumed to have been observed by applying the criteria $I \ge 2\sigma(I)$. For compound **2**, 1751 reflections were measured in the range $2.8 \le \theta \le 30°$, 1638 of which are considered to have been observed applying the condition $I \ge 2\sigma(I)$. In the case of compound **3**, 2669 reflections were measured in the range $2 \le \theta \le 30°$, of which 1267 reflections were assumed to be observed applying the criteria $I \ge 2\sigma(I)$. Correction for Lorentz and polarization effects were done, but not for absorption. The program employed to solve the three structures was SHELX86.[15] They were then refined by the full-matrix least-squares method, using the SHELX93[16] computer program. The scattering factors were taken from ref 17. All non-hydrogen atoms were assigned anisotropic thermal parameters. H positions were obtained from difference Fourier syntheses for compounds **1**−**3**. The final *R* factors were $R(F_o) = 0.029$ ($wR(F_o^2) = 0.078$) for compound **1**, $R(F_o) = 0.025$ ($wR(F_o^2) = 0.060$) for compound **2**, and $R(F_o) = 0.029$ ($wR(F_o^2) = 0.069$) for compound **3**. Maximum and minimum peaks in final difference synthesis were 0.61, −0.32, 0.24, −0.28, and 0.64, −0.30 e $Å^{-3}$ for compounds **1**−**3**, respectively. The final atomic positional parameters for the non-hydrogen atoms of the compounds are listed together in Table 2.

**Table 1.** Crystal Data and Structure Refinement for Compounds **1**−**3**

| | compound | | |
|---|---|---|---|
| | **1** | **2** | **3** |
| chem formula | $C_{14}H_9N_8S_2Mn$ | $C_{10}H_6N_6O_2Mn$ | $C_4H_3N_8Mn$ |
| *a*, Å | 9.122(1) | 7.309(1) | 6.206(2) |
| *b*, Å | 9.229(1) | 14.498(2) | 15.084(2) |
| *c*, Å | 11.710(2) | 10.740(4) | 8.909(1) |
| α, deg | 74.89(1) | | |
| *β*, deg | 80.30(1) | 99.93(4) | 95.75(2) |
| *γ*, deg | 61.04(1) | | |
| *V*, $Å^3$ | 831.7(2) | 1121.0(5) | 829.8(3) |
| *Z* | 2 | 4 | 4 |
| fw | 408.35 | 297.15 | 218.08 |
| space group | $P\bar{1}$ (No. 2) | *C*2/*c* (No. 15) | *C*2/*m* (No. 12) |
| *T*, °C | 293(2) | 293(2) | 293(2) |
| $\rho_{obsd}$, g $cm^{-3}$ | 1.61(2) | 1.76(2) | 1.73(2) |
| $\rho_{calcd}$, g $cm^{-3}$ | 1.63 | 1.76 | 1.75 |
| $\mu$, $cm^{-1}$ | 10.6 | 11.85 | 15.54 |
| $\lambda$, Å | 0.710 69 | 0.710 69 | 0.710 69 |
| $R(F_o)^a$ | 0.029 | 0.025 | 0.029 |
| $R_w(F_o^2)^b$ | 0.078 | 0.060 | 0.069 |

[a] $R(F_o) = [\sum|\Delta F|/\sum|F_o|]$. [b] $R_w(F_o^2) = [\sum\{w(\Delta F^2)^2\}/\sum\{w(F_o^2)^2\}]^{1/2}$.

## Results and Discussion

**Description of the Structure of $[Mn_2(bpm)_3(NCS)_4]$ (1).** The structure of this compound consists of centrosymmetric discrete dinuclear units formulated $[Mn_2(bpm)_3(NCS)_4]$. In these units, the manganese(II) ions are bridged by a bpm ligand in a bis-bidentate fashion. The Mn···Mn intramolecular separation is 6.2117(3) Å. A perspective view of the molecule with the labeling of the atoms is shown in Figure 1. Each manganese atom is bound to six nitrogen atoms belonging to two $NCS^-$ groups in a *cis* position and two bpm ligands, one being terminal and the other being bridging. Selected bond distances and angles for this complex are given in Table 3. The Mn−N bond lengths involving bpm ligands [Mn−N(1),N(2)$^I$,N(3),N(5); 2.302(2), 2.395(2), 2.277(2), 2.261(2) Å; $I = 1 - x, 1 - y, 1 - z$] are larger than those involving thiocyanate ligands [Mn−N(7),N(8); 2.129(2), 2.107(2) Å]. The distortion of the octahedral geometry has been evaluated using the Muetterties and Guggenberger description[18] to give a Δ value next to 0.26 for the compound (Supporting Information), which indicates a high distortion from the ideal topology.

(13) (a) Julve, M; De Munno, G.; Bruno, G.; Verdaguer, M. *Inorg. Chem.* **1988**, *27*, 3160. (b) Julve, M.; Verdaguer, M.; De Munno, G.; Real, J. A.; Bruno, G. *Inorg. Chem.* **1993**, *32*, 795. (c) De Munno, G.; Julve, M.; Verdaguer, M.; Bruno, G. *Inorg. Chem.* **1993**, *32*, 2215.
(14) De Munno, G.; Julve, M.; Nicoló, F.; LLoret, F.; Faus, J.; Ruiz, R.; Sinn, E. *Angew. Chem., Int. Ed. Engl.* **1993**, *32*, 613.
(15) Sheldrick, G. M. SHELX 86. *Acta Crystallogr.* **1990**, *A46*, 467.
(16) Sheldrick, G. M. SHELX 93. *J. Appl. Crystallogr.* **1996**, in press.
(17) *International Tables for X-ray Crystallography*; Kynoch: Birmingham, England, 1974; Vol. IV, p 99.
(18) Muetterties, E. L.; Guggenberger, L. J. *J. Am. Chem. Soc.* **1974**, *96*, 1748.

**Table 2.** Selected Atomic Coordinates and Equivalent Isotropic Thermal Parameters

| atom | *x*/*a* | *y*/*b* | *z*/*c* | $U_{eq}$,[a] Å$^2$ |
|---|---|---|---|---|
| | | Compound **1** | | |
| Mn | 2809(1) | 7643(1) | 2931(1) | 28(1) |
| S(1) | −2302(1) | 7268(1) | 4274(1) | 47(1) |
| S(2) | 1466(1) | 7153(1) | −744(1) | 55(1) |
| C(1) | 5119(2) | 3636(2) | 2964(2) | 31(1) |
| C(2) | 6073(3) | 1955(3) | 3454(2) | 34(1) |
| C(3) | 6555(2) | 1556(2) | 4588(2) | 33(1) |
| C(4) | 5230(2) | 4332(2) | 4665(1) | 23(1) |
| N(1) | 4669(2) | 4842(2) | 3577(1) | 26(1) |
| N(2) | 6159(2) | 2742(2) | 5206(1) | 27(1) |
| N(3) | 4875(2) | 8246(2) | 1919(1) | 31(1) |
| N(5) | 1971(2) | 10427(2) | 2770(1) | 30(1) |
| C(13) | −641(2) | 7536(2) | 4002(2) | 33(1) |
| C(14) | 2053(3) | 7131(2) | 492(2) | 35(1) |
| N(7) | 525(2) | 7768(2) | 3818(2) | 46(1) |
| N(4) | 5766(2) | 10370(2) | 1267(2) | 41(1) |
| C(5) | 6288(3) | 7159(3) | 1438(2) | 39(1) |
| C(8) | 4671(2) | 9818(2) | 1783(2) | 30(1) |
| N(8) | 2443(3) | 7136(2) | 1377(2) | 48(1) |
| C(10) | 489(3) | 11524(3) | 3195(2) | 37(1) |
| N(6) | 2750(2) | 12628(2) | 2117(2) | 43(1) |
| C(9) | 3030(2) | 11044(2) | 2252(2) | 30(1) |
| C(6) | 7502(3) | 7609(3) | 884(2) | 44(1) |
| C(7) | 7199(3) | 9221(3) | 833(2) | 46(1) |
| C(11) | 100(3) | 13169(3) | 3107(2) | 42(1) |
| C(12) | 1265(3) | 13680(3) | 2556(2) | 47(1) |
| | | Compound **2** | | |
| Mn | 0 | 1089(1) | 2500 | 31(1) |
| N(1) | 1606(2) | 816(1) | 817(2) | 32(1) |
| N(2) | −1473(2) | −69(1) | 1167(2) | 31(1) |
| C(1) | −853(3) | −242(1) | 95(2) | 26(1) |
| C(2) | 3131(3) | 1268(2) | 619(2) | 47(1) |
| C(3) | −3860(4) | −1154(2) | 462(3) | 59(1) |
| C(4) | −2994(3) | −531(2) | 1339(2) | 46(1) |
| N(3) | 2140(3) | 2000(1) | 3209(2) | 60(1) |
| C(5) | 2811(4) | 2693(2) | 3478(2) | 43(1) |
| O(1) | 3966(10) | 3277(6) | 3775(9) | 87(2) |
| O(1′) | 3079(9) | 3507(5) | 3725(8) | 62(2) |
| | | Compound **3** | | |
| Mn | 5000 | 7027(1) | 0 | 21(1) |
| N(1) | 5956(4) | 5784(1) | 1424(2) | 24(1) |
| N(2) | 7218(4) | 7874(2) | 1383(3) | 31(1) |
| N(3) | 7023(5) | 8236(2) | 2536(3) | 45(1) |
| N(4) | 6860(8) | 8578(4) | 3654(5) | 103(2) |
| C(1) | 6825(5) | 5778(2) | 2849(3) | 29(1) |
| C(2) | 7248(8) | 5000 | 3633(4) | 35(1) |
| C(3) | 5526(6) | 5000 | 776(4) | 20(1) |

[a] $U_{eq}$ is defined as one-third the trace of the orthogonalized $\mathbf{U}_{ij}$ tensor.

Whereas the NCS groups are quasi-linear [N(7)−C(13)−S(1) = 178.2(2)° and N(8)−C(14)−S(2) = 178.8(2)°], the Mn−N−C(S) linkages are significantly bent [Mn−N(7)−C(13) = 156.2(2)° and Mn−N(8)−C(14) = 168.9(2)°]. The shortest intermolecular Mn···Mn separation is equal to 7.0504(3) Å.

**Description of the Structure of [Mn(bpm)(NCO)$_2$] (2).** The structure of this compound consist of linear chains in which the manganese(II) ions are bridged by *cis* bpm ligands in the bis-bidentate form. The metal centers are related by glide-plane symmetry. The intramolecular Mn···Mn distance is 6.2296(3) Å, whereas the shortest interchain distance is 7.2224(3) Å. The other two sites of a distorted octahedral coordination sphere are occupied by terminal cyanate ligands (Figure 2). Selected bond distances and angles for this complex are given in Table 4. The Mn−N distances corresponding to the bridging bpm ligands [Mn−N(1),N(1)$^I$,N(2),N(2)$^I$; 2.352(2), 2.352(2), 2.345(2), 2.345(2) Å; I = $-x$, $y$, $^1/_2 - z$] are larger again than those involving the cyanate ligands [Mn−N(3),N(3)$^I$; 2.089(2), 2.088(2) Å], which are also in *cis* arrangement. The distortion of the octahedral geometry gives a Δ value next to 0.28.

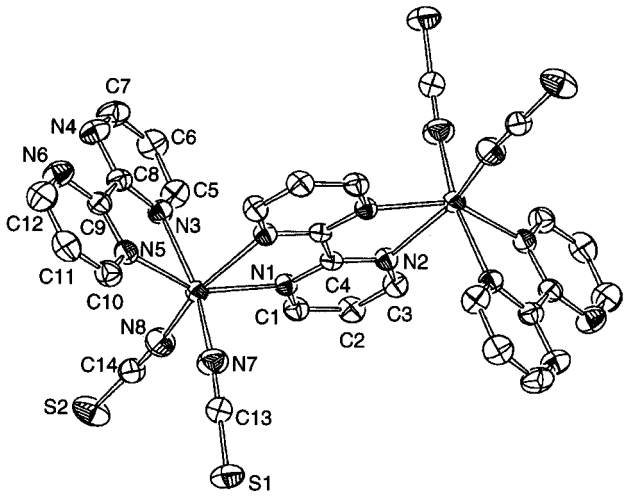


**Figure 1.** ORTEP view of the dinuclear [Mn$_2$(bpm)$_3$(NCS)$_4$] compound, together with the atom labeling.

**Table 3.** Selected Bond Distances (Å) and Angles (deg) for [Mn$_2$(bpm)$_3$(NCS)$_4$][a]

| | | | |
|---|---|---|---|
| Mn−N(1) | 2.302(2) | Mn−N(8) | 2.107(2) |
| Mn−N(2)$^I$ | 2.395(2) | S(1)−C(13) | 1.618(2) |
| Mn−N(3) | 2.277(2) | S(2)−C(14) | 1.618(2) |
| Mn−N(5) | 2.261(2) | C(13)−N(7) | 1.159(3) |
| Mn−N(7) | 2.129(2) | C(14)−N(8) | 1.153(3) |
| N(8)−Mn−N(7) | 95.07(8) | N(8)−Mn−N(2)$^I$ | 161.36(7) |
| N(8)−Mn−N(5) | 112.16(7) | N(7)−Mn−N(2)$^I$ | 89.50(7) |
| N(7)−Mn−N(5) | 93.80(7) | N(5)−Mn−N(2)$^I$ | 85.48(5) |
| N(8)−Mn−N(3) | 88.58(7) | N(3)−Mn−N(2)$^I$ | 91.56(6) |
| N(7)−Mn−N(3) | 165.26(7) | N(1)−Mn−N(2)$^I$ | 69.85(5) |
| N(5)−Mn−N(3) | 71.64(6) | N(7)−C(13)−S(1) | 178.2(2) |
| N(8)−Mn−N(1) | 91.52(7) | N(8)−C(14)−S(2) | 178.8(2) |
| N(7)−Mn−N(1) | 101.65(6) | C(13)−N(7)−Mn | 156.2(2) |
| N(5)−Mn−N(1) | 150.50(5) | C(14)−N(8)−Mn | 168.9(2) |
| N(3)−Mn−N(1) | 92.50(6) | | |

[a] Symmetry transformations used to generate equivalent atoms: I = $-x + 1$, $-y + 1$, $-z + 1$.

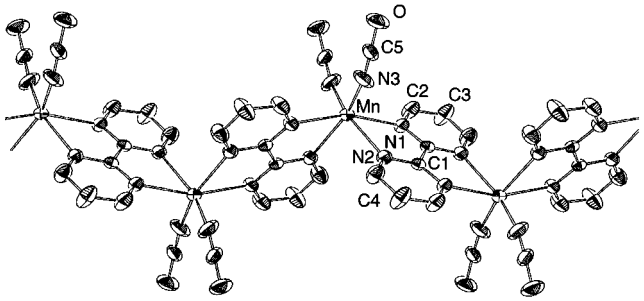


**Figure 2.** Arrangement of the [Mn(bpm)(NCO)$_2$] chains, together with the atom labeling.

The oxygen atoms of the cyanate ligands are disordered (O(1), O(1′), being assigned occupation factors of 0.5. The Mn−N−C(O) linkages are significantly bent (Mn−N(3)−C(5) = 156.6(2)°).

**Description of the Structure of [Mn$_2$(bpm)(N$_3$)$_4$] (3).** The whole structure of compound **3** can be described as parallel honeycomb-like sheets, each consisting of an infinite hexagonal array of manganese(II) ions bridged by bis-bidentate bpm ligands and double EO azido bridges. This 2D compound extends in the *xy* plane by repetition of edge-sharing hexagons, as shown in Figure 3. Selected bond distances and angles for this complex are given in Table 5. The manganese(II) ion exhibits a highly distorted octahedral environment formed by

**Table 4.** Selected Bond Distances (Å) and Angles (deg) for $[Mn(bpm)(NCO)_2]$[a]

| | | | |
|---|---|---|---|
| Mn−N(1)$^{I}$ | 2.352(2) | Mn−N(3) | 2.089(2) |
| Mn−N(1) | 2.352(2) | N(3)−C(5) | 1.132(3) |
| Mn−N(2) | 2.345(2) | C(5)−O(1) | 1.200(8) |
| Mn−N(2)$^{I}$ | 2.345(2) | C(5)−O(1′) | 1.219(7) |
| Mn−N(3)$^{I}$ | 2.088(2) | | |
| N(3)$^{I}$−Mn−N(3) | 101.53(14) | N(2)$^{I}$−Mn−N(1)$^{I}$ | 69.37(6) |
| N(3)$^{I}$−Mn−N(2) | 89.65(8) | N(3)$^{I}$−Mn−N(1) | 105.53(7) |
| N(3)−Mn−N(2) | 155.77(8) | N(3)−Mn−N(1) | 86.84(8) |
| N(3)$^{I}$−Mn−N(2)$^{I}$ | 155.77(8) | N(2)−Mn−N(1) | 69.37(6) |
| N(3)−Mn−N(2)$^{I}$ | 89.65(8) | N(2)$^{I}$−Mn−N(1) | 96.41(6) |
| N(2)−Mn−N(2)$^{I}$ | 88.54(9) | N(1)$^{I}$−Mn−N(1) | 160.65(8) |
| N(3)$^{I}$−Mn−N(1)$^{I}$ | 86.84(8) | C(5)−N(3)−Mn | 156.6(2) |
| N(3)−Mn−N(1)$^{I}$ | 105.53(7) | N(3)−C(5)−O(1) | 161.4(5) |
| N(2)−Mn−N(1)$^{I}$ | 96.41(6) | N(3)−C(5)−O(1′) | 163.9(4) |

[a] Symmetry transformations used to generate equivalent atoms: I = $-x$, $y$, $-z + {}^1/_2$.

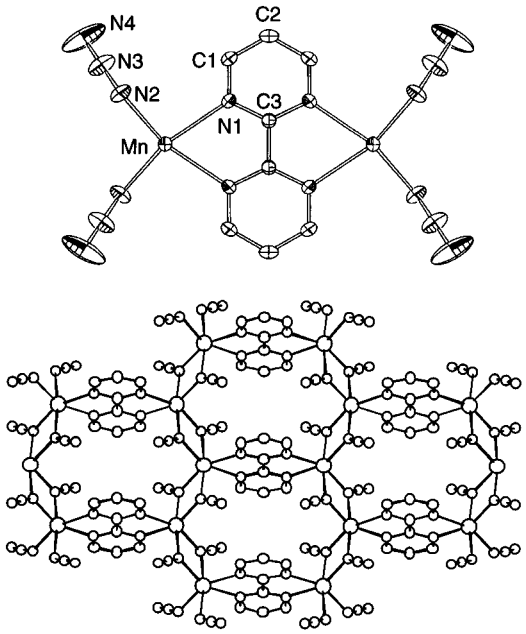


**Figure 3.** (a) Top: ORTEP view, with the atom labeling, of the $[Mn_2(bpm)(N_3)_4]$ compound. (b) Bottom: View of the sheet in the *xy* plane.

six nitrogen atoms, four of the azido [Mn−N(2),N(2)$^{I}$,N(2)$^{II}$, N(2)$^{III}$; 2.169(2), 2.169(2), 2.225(2), 2.225(2) Å; I = $-x + 1$, $y$, $-z$; II = $-x + {}^3/_2$, $-y + {}^3/_2$, $-z$; III = $x - {}^1/_2$, $-y + {}^3/_2$, $z$] and two of the bpm [Mn−N(1),N(1)$^{I}$; 2.308(2), 2.308(2) Å], respectively. The axial azide bond lengths are longer than the equatorial ones, and all of them are shorter than those involving bpm. The double EO azido bridges form the same angle with the metal, having a value of 102.01(9)°. The Mn···Mn distances through the azido-bridged $Mn(N_3)_2Mn$ unit and the bpm ligand are 3.425(4) and 6.127(2) Å, respectively.

In all complexes the bpm ligands may be considered as rigid and quasi-planar. The average C−C and C−N bond distances in the rings of this ligand are 1.42(1) and 1.35(1) Å for compounds **1**−**3**. These values are in good agreement with those currently given in the literature for this ligand.[19−21]

**Infrared Spectroscopy.** The most important aspects containing the infrared spectra of **1**−**3** deal with the possibility to distinguish between the chelating and bis-chelating coordination modes of bpm and to characterize the presence of the different coordination modes of the pseudohalide ligands. Infrared spectra provide a good test to recognize a compound with a terminal (chelating) bpm ligand.[13] The spectrum then exhibits the ring stretching mode of bpm as a sharp and characteristic band at 1565 cm$^{-1}$, which is associated with another at 1580 cm$^{-1}$ forming a quasi-symmetric doublet. The first band does not exist when bpm is only bridging (bis-chelating), and the ring stretching mode appears as a very asymmetric doublet at 1580 cm$^{-1}$.[13]

**Table 5.** Selected Bond Distances (Å) and Angles (deg) for $[Mn_2bpm(N_3)_4]$[a]

| | | | |
|---|---|---|---|
| Mn−N(1) | 2.308(2) | Mn−N(2)$^{III}$ | 2.225(2) |
| Mn−N(1)$^{I}$ | 2.308(2) | N(2)−N(3) | 1.180(3) |
| Mn−N(2) | 2.169(2) | N(2)−Mn$^{II}$ | 2.225(2) |
| Mn−N(2)$^{I}$ | 2.169(2) | N(3)−N(4) | 1.135(4) |
| Mn−N(2)$^{II}$ | 2.225(2) | | |
| N(2)$^{I}$−Mn−N(2) | 107.81(14) | N(2)$^{I}$−Mn−N(1)$^{I}$ | 93.04(9) |
| N(2)$^{I}$−Mn−N(2)$^{II}$ | 97.44(9) | N(2)−Mn−N(1)$^{I}$ | 154.74(9) |
| N(2)−Mn−N(2)$^{II}$ | 77.99(9) | N(2)$^{II}$−Mn−N(1)$^{I}$ | 85.47(8) |
| N(2)$^{I}$−Mn−N(2)$^{III}$ | 77.99(9) | N(2)$^{III}$−Mn−N(1)$^{I}$ | 100.80(9) |
| N(2)−Mn−N(2)$^{III}$ | 97.44(9) | N(1)−Mn−N(1)$^{I}$ | 71.30(11) |
| N(2)$^{II}$−Mn−N(2)$^{III}$ | 172.34(12) | N(3)−N(2)−Mn | 130.7(2) |
| N(2)$^{I}$−Mn−N(1) | 154.74(9) | N(3)−N(2)−Mn$^{II}$ | 127.2(2) |
| N(2)−Mn−N(1) | 93.04(9) | Mn−N(2)−Mn$^{II}$ | 102.01(9) |
| N(2)$^{II}$−Mn−N(1) | 100.81(9) | N(4)−N(3)−N(2) | 179.1(4) |
| N(2)$^{III}$−Mn−N(1) | 85.47(8) | | |

[a] Symmetry transformations used to generate equivalent atoms: I = $-x + 1$, $y$, $-z$; II = $-x + {}^3/_2$, $-y + {}^3/_2$, $-z$; III = $x - {}^1/_2$, $-y + {}^3/_2$, $z$.

The IR spectrum of compound **1** shows a quasi-symmetric doublet containing the band associated with terminal bpm groups. This band does not appear for complexes **2** and **3**, indicating the presence of bis-chelating bpm only for both compounds.[13]

The $\nu_{as}$(NCX) stretching mode of the pseudohalide ions, located in the region of 2000 cm$^{-1}$, is very useful to determine the nature of the coordination modes of the thiocyanate, cyanate, and azido groups. In the present case, the $\nu$(CN) stretching vibration of the NCS group appears as a single intense band at 2100 cm$^{-1}$ for compound **1**. This frequency suggests a terminal coordination of thiocyanate groups, in good accordance with the structural results. The $\nu$(CS) stretching vibration appears at 785 cm$^{-1}$. In compound **2**, the $\nu_{as}$(NCO) appears as a single and intense band at 2200 cm$^{-1}$, which is in agreement with monodentate coordination for cyanate groups through its N atom.[22] Finally, the $\nu_{as}(N_3)$ vibration mode appears as a doublet at 2100 and 2075 cm$^{-1}$ for compound **3**. This fact, together with the occurrence of a weak band at about 1300 cm$^{-1}$, corresponding to the $\nu_s(N_3)$ vibration mode, supports the presence of end-on azido bridges[1a] as confirmed by the crystal structure of this compound.

**EPR Spectra and Magnetic Properties.** The X-band EPR spectra of compounds **1**−**3** show isotropic signals with $g$ values of 2.0. For compounds **1** and **2**, a weak $\Delta M_s = 2$ forbidden transition is also observed at room temperature, while their spectra remain practically unchanged on cooling to liquid nitrogen. For compound **3**, the signal increases in intensity and narrows upon cooling to liquid nitrogen.

The thermal variation of magnetic susceptibility, in the form of $\chi_m$ vs $T$, for both compounds **1** and **2** are shown together in Figure 4. The molar susceptibility value ($2.79 \times 10^{-2}$ cm$^3$ mol$^{-1}$ for **1** and $1.40 \times 10^{-2}$ cm$^3$ mol$^{-1}$ for **2** at room

(19) De Munno, G.; Bruno, G. *Acta Crystallogr., Sect. C*: *Cryst. Struct. Commun*. **1984**, *C40*, 2030.
(20) Julve, M.; De Munno, G.; Bruno, G.; Verdaguer, M. *Inorg. Chem.* **1988**, *27*, 3160.
(21) Morgan, L. W.; Goodwin, K. V.; Pennington, W. T.; Petersen, J. D. *Inorg. Chem.* **1992**, *31*, 1103.
(22) Lever, A. B. P.; Mantovani, E.; Ramaswamy, B. S. *Can. J. Chem.* **1971**, *49*, 1957.

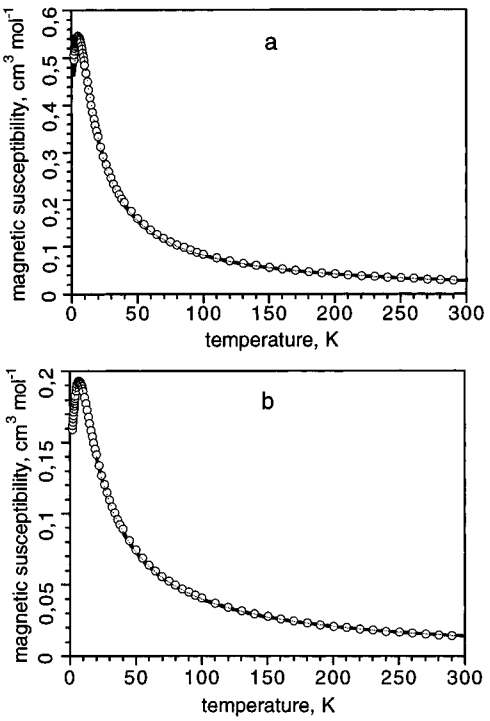


**Figure 4.** Thermal variations of the Magnetic susceptibility ($\chi_m$) for (a) $[Mn_2(bpm)_3(NCS)_4]$ and (b) $[Mn(bpm)(NCO)_2]$ compounds. Solid curves represent the best fit to the theoretical models.

temperature) increases upon cooling, reaching a maximum of $5.46 \times 10^{-1}$ cm$^3$ mol$^{-1}$ at 5 K and $1.93 \times 10^{-1}$ cm$^3$ mol$^{-1}$ at 7 K for **1** and **2**, respectively, and then rapidly decreases. The $\chi_m T$ value decreases from 8.39 cm$^3$ K mol$^{-1}$ (300 K) to 0.89 cm$^3$ K mol$^{-1}$ (1.8 K) for two manganese(II) ions in **1** and from 4.20 cm$^3$ K mol$^{-1}$ (300 K) to 0.29 cm$^3$ K mol$^{-1}$ (1.8 K) for one manganese(II) ion in **2**, tending to zero. Both the continuous decrease in the $\chi_m T$ value and the maximum observed in the thermal variation of the molar susceptibility clearly indicate the existence of intramolecular antiferromagnetic interactions in both compounds **1** and **2**.

To interpret quantitatively the magnetic data for compound **1**, we can analyze them in terms of the "dipolar coupling" approach for a Mn(II) dinuclear compound. The expression for the magnetic susceptibility of the manganese(II) dimer, derived from Van Vleck's equation, using the Hamiltonian $H = -2J\hat{S}_1\hat{S}_2$, is

$$\chi_A = \frac{3N\beta^2 g^2}{3kT}[(55 + 30\exp(10X) + 14\exp(18X) + 5\exp(24X) + \exp(28X))/(11 + 9\exp(10X) + 7\exp(18X) + 5\exp(24X) + 3\exp(28X) + \exp(30X))] \quad (1)$$

with $X = -J/kT$.

The fit following the above expression allows an evaluation of the intradimer exchange integral $J$ for the compound. The calculated solid line in Figure 4a shows excellent agreement with the observed values (circles), providing the parameter $J = -0.72$ K, with $g = 2.0$, as obtained from the EPR measurements. The agreement factor, defined as $SE = [\Phi/(n - K)]^{1/2}$, where $n$ is the number of data points, $K$ is the number of adjustable parameters (1), and $\Phi = \Sigma[\chi_m T_{obs} - \chi_m T_{calc}]^2$ is the sum of squares of the residuals, is equal to $2.8 \times 10^{-4}$, which actually corresponds to an excellent experiment-theory agreement.

The magnetic behavior of **2** was analyzed by fitting the experimental susceptibility to Fisher's calculation[23] for a classical or infinite spin linear chain, scaled to a real spin of $^5/_2$.[24] The expression for the magnetic susceptibility of the manganese(II) chain is

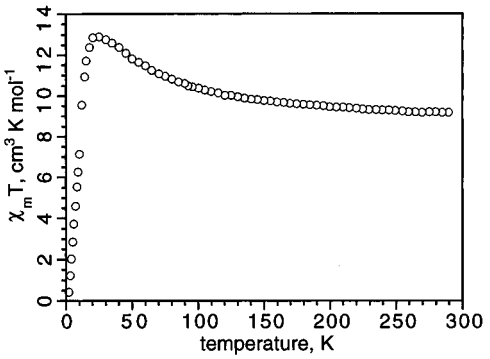


**Figure 5.** Thermal variation of $\chi_m T$ for the $[Mn_2(bpm)(N_3)_4]$ compound.

$$\chi = \frac{Ng^2\beta^2 S(S+1)}{3kT}\frac{1-u}{1+u} \quad (2)$$

where $u = (T/T_0) - \coth(T_0/T)$ with $T_0 = 2JS(S + 1)/k$.

The best fit result, Figure 4b, leads to $J = -0.78$ K. The $g$ factor was taken equal to 2.0 as obtained from the EPR measurements. The agreement factor using the above expression was $3.9 \times 10^{-4}$, showing an excellent theory−experiment agreement.

The thermal variation of the molar magnetic susceptibility $\chi_m$ for compound **3** shows that $\chi_m$ gradually increases upon cooling, reaching a sharp maximum near 12 K after which it rapidly decreases. The maximum observed is indicative of the existence of antiferromagnetic interactions at temperatures lower than 12 K. The $\chi_m T$ vs $T$ curve for this compound is shown in Figure 5. The room-temperature value of $\chi_m T$ is 9.19 cm$^3$ mol$^{-1}$ K, which is slightly higher than that calculated for two noninteracting manganese(II) ions (8.76 cm$^3$ mol$^{-1}$ K). The initial rise in $\chi_m T$ with decreasing temperature indicates the dominant role of the ferromagnetic interaction. However $\chi_m T$ reaches a maximum of 12.90 cm$^3$ mol$^{-1}$ K near 20 K and then rapidly descends. Such a turnover indicates weaker antiferromagnetic interactions are also present in the material. Both kinds of interaction are supported by the simultaneous existence of bpm (transmitting antiferromagnetic interactions) and end-on azido ligands (transmitting ferromagnetic interactions). In fact, the Mn−bpym−Mn fragment in the compound is similar to that found in the dinuclear $[Mn_2(bpym)(H_2O)_6(SO_4)_2]$ compound[14] which exhibits antiferromagnetic interactions with $J = -1.1$ cm$^{-1}$. On the other hand, ferromagnetic coupling through end-on azido bridges in manganese compounds has also been observed in one dinuclear $[Mn(terpy)(N_3)_2]_2 \cdot 2H_2O$ and in one 1D $[Mn(bpy)(N_3)_2]$ compounds showing $J = +1.5$ and $+2.5$ cm$^{-1}$, respectively.[1a,b]

Two-dimensional compounds exhibiting alternating sign magnetic interactions are extremely rare. One example of this kind may be considered the $(PDA)Cu(ox)_2$ complex (where PDA = propylenediammonium and ox= oxalate). This compound shows a molecular structure consisting of a linear chain arrangement of the $Cu(ox)_2^{2-}$ anions. However, the chains pack together in layers, held by hydrogen bonds through the countercations, and show ferromagnetic intrachain and antiferro-

(23) Fisher, M. E. *Am. J. Phys.* **1964**, *32*, 343.
(24) Dingle, R.; Lines, M. E.; Holt, S. L. *Phys. Rev.* **1969**, *187*, 643.

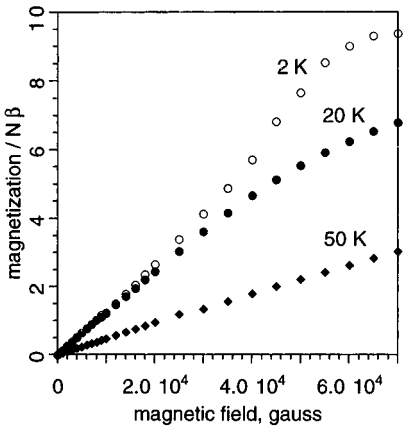


**Figure 6.** Magnetization vs magnetic field, at different temperatures, for the $[Mn_2(bpm)(N_3)_4]$ compound.

magnetic interchain coupling.[25] To our knowledge, compound **3** represents the first example of a 2D "honeycomb-like" molecular compound having alternating sign magnetic interactions. The lack of a theoretical model for an alternating sign magnetic plane of this kind does not allow us to get the actual values for the magnetic exchange parameters. However, in order to make an estimation of the magnitude of the magnetic couplings, an attempt has been made to fit the magnetic data to the prediction for the susceptibility of a ferromagnetic linear chain of Heisenberg-coupled $S = {}^5/_2$ atoms with an antiferromagnetic parameter introduced with the molecular field approximation.[23] The best result gives $J \approx +2$ cm$^{-1}$ and $zJ' \approx -0.5$ cm$^{-1}$. These values are indicative of the relative strength of the interactions, but the fit is not good enough to take them as realistic values. Even a moderately good fit to this model can be obtained with the parameters $J = -1.06$ cm$^{-1}$ and $zJ' = +1.99$ cm$^{-1}$, obviously incorrect taking into account the model used and the exchange pathways available in the complex.

The magnetization data for compound **3** show an anomalous behavior at low temperatures and high magnetic fields (see Figure 6). At 2 K, the magnetization rapidly increases for magnetic fields higher than 1 T and practically reaches the saturation value at 7 T. This behavior is also observed at higher temperatures, although the saturation value is not reached above 10 K. This unexpected behavior for an antiferromagnetic ordered system could be due, in principle, to a metamagnetism phenomenon owing to the existence of competitive ferro- and antiferromagnetic interactions in the compound. However, the observed saturation without a first-order transition does not fully corroborate this hypothesis. Measurements at lower temperatures and/or oriented samples are needed to a complete analysis of this behavior.

## Discussion

The same synthetic method aimed to achieve the connection of Mn(II)−pseudohalide systems through bpm ligands has surprisingly led to different dinuclear (NCS), one-dimensional (NCO), and two-dimensional ($N_3$) species. In the two former systems, the manganese(II) ions are connected through bpm bridges, whereas in the latter EO azido and bpm bridges are present. The influence of every pseudohalide ligand has then been dramatic for the final molecular structure and as a consequence for the magnetic properties. It has again been demonstrated the greater versatility for coordinating of the azido ligand with respect to the cyanate and thiocyanate ones. For compounds **1** and **2** antiferromagnetic couplings are observed. In this sense, the bis-bidentate bpm ligands have a specific ability to favor an antiferromagnetic interaction between metal centers, provided that a magnetic orbital of *xy* symmetry is available on each interacting ion.[26] Such an *xy*-exchange pathway is operative with manganese(II). From both structural and magnetic points of view, the most interesting compound is actually **3**, where both alternating ferro- (through EO azide) and antiferromagnetic (through bpm) interactions are present. The bridging angle corresponding to the EO azido bridges [102.01(9)°] in compound **3** is similar to those observed in $[Mn(terpy)(N_3)_2]_2 \cdot 2H_2O$ [104.6(2)°][1a] and $[Mn(bpy)(N_3)_2]$ [101.0(2)°][1b] compounds, which show ferromagnetic interactions. As a consequence, a ferromagnetic exchange coupling constant in the range $2-10$ cm$^{-1}$ is to be expected for this compound. It constitutes the first two-dimensional honeycomb-like compound in which the magnetic interactions alternate in sign.

**Acknowledgment.** This work has been carried out with the financial support of the Universidad del Pais Vasco/Euskal Herriko Unibertsitatea (Grant UPV 130.310.EB234/95) and the Dept. Educación, Universidades e Investigación, Gobierno Vasco/Eusko Jaurlaritza (Grant PI 96/39), which we gratefully acknowledge.

**Supporting Information Available:** Listings of structural determination data, anisotropic displacement parameters, bond distances and angles, torsion angles, and molar magnetic susceptibility vs temperature data (26 pages). Ordering information is given on any current masthead page.

IC960969H

(25) Bloomquist, D. R.; Hansen, J. J.; Landee, C. P.; Willett, R. D.; Buder, R. *Inorg. Chem.* **1981**, *20*, 3308.

(26) Kahn, O. *Angew. Chem., Int. Ed. Engl.* **1985**, *24*, 834.